2015

# Brain volumetric MRI study of extremely low gestational age newborns (ELGANs) at 9 to 10 years of age

BOSTON UNIVERSITY

SCHOOL OF MEDICINE

Thesis

# BRAIN VOLUMETRIC MRI STUDY OF EXTREMELY LOW GESTATIONAL AGE NEWBORNS (ELGANs) AT 9 TO 10 YEARS OF AGE

by

**QINGDE ZHOU**

M.D., Hunan Medical University, 1988

Submitted in partial fulfillment of the

requirements for the degree of

Master of Science

2015

**Approved by**

**First Reader:** _____

Hernán Jara, Ph.D.
Professor of Radiology

**Second Reader:** _____

Ronald J. Killiany, Ph.D.
Associate Professor

## ACKNOWLEDGEMENTS

Throughout the past three years, I have received support and encouragement from a number of people. First, I would like to thank Dr. Hernan Jara. He has become a mentor, colleague, and friend of mine. As I moved from an idea to a completed study, his guidance has made this a thoughtful and rewarding journey. In addition, I greatly appreciate Adam Aakil, Khalid M. Alshamrani, and Dong Hyun Hong. They spent countless hours to train me on image preparation and segmentation. I would like to thank Dr. Ronald J. Killiany who read my thesis and gave me valuable suggestions, and thank other teachers who took part in my study for generously sharing their time and ideas. I have learned much through our conversations. Finally, I thank my wife Xiaoyan Tan. She has always had faith in my abilities and supported me for the Bioimaging study. She has taken the full responsibilities for our children's education and for most of the housework in our family during my study. Without her support, it is impossible for me to complete the Master of Bioimaging program successfully while keep my full time biomedical research job at the same time. I am thankful for my two daughters, Baiyu and Baifan Zhou. They always make me happy and feel relaxed at home. They have helped me with housework, and have always understood me when I had no time to help with their homework or to play with them.

*The ELGAN Study is supported by the National Institute of Neurological Disorders and Stroke (NS040069)*

**BRAIN VOLUMETRIC MRI STUDY OF EXTREMELY LOW GESTATIONAL AGE NEWBORNS (ELGANs) AT 9 TO 10 YEARS OF AGE**

**QINGDE ZHOU**

ABSTRACT

**Purpose:** Extremely low gestation age newborns (ELGANs) are at high risk for developmental brain abnormalities, which can lead to cognitive, physical, emotional and behavioral deficits. This study is to determine potential brain volumetric abnormalities of ELGAN children at 9 to 10 years of age.

**Methods**: High-resolution magnetic resonance imaging (MRI) scans were obtained from 82 ELGAN children using a dual-echo turbo spin-echo (DE-TSE) pulse sequence at 3.0T (or 1.5T at only one site). The DICOM MR images were processed with quantitative MRI algorithms programmed in Mathcad. The brain gray matter (GM), white matter (WM) and cerebrospinal fluid (CSF) volumes were quantified using semi-automated clustering segmentation algorithms.

**Results:** Total brain volumes (GM+WM) of ELGAN children showed a large distribution range from 400 to 1500 mL. About 63% of the children had smaller brain volumes while 5% of them had larger brain volumes compared to the published data from normal children at the same ages[1]. Smaller brain volumes were observed more often in males (74%) than in females (50%). WM reduction was the major change in ELGANs with over 90% of them (86% of males and 92% of females) having reduced WM volumes. GM volumes were either reduced (15%) or enlarged (32%); GM reduction was

observed more often in males (31%) than in females (4.8%), while GM enlargement was more frequently observed in females (35%) than in males (28%). Intracranial CSF volumes range from 25 mL to 600 mL, with 16% of ELGAN children (9% of males and 21% of females) having smaller CSF volume, while 38% of them (53% of males and 27% of females) having larger CSF volume. Correlation analysis revealed a positive correlation between total intracranial matter (ICM) and CSF volumes (male: r = 0.4972, $p$ = 0.0014 and female: r = 0.3233, $p$ = 0.0125), but a negative correlation was found between brain volumes and CSF volumes (male: r = - 0.2998, $p$ = 0.0424 and female: r = - 0.2279, $p$ = 0.0596). Further analysis demonstrated a negative correlation between GM and CSF both in absolute (male: r = - 0.4489, $p$ = 0.0039 and female: r = - 0.3769, $p$ = 0.0041) and in relative (male: r = - 0.8675, $p$ = 0.0000 and female: r = - 0.8350, $p$ = 0.0000) volumes, while WM volumes did not correlate with CSF volumes.

**Conclusion:** ELGAN children had mostly smaller brain volumes while some of them displayed larger brain volumes at ages of 9 to 10 years. The reduction of WM was a characteristic change in ELGAN children and contributed to smaller brain volumes. GM volumes either increased or decreased. Larger intracranial CSF volumes were associated with larger intracranial matter (ICM) volume.

## TABLE OF CONTENTS

Page

## LIST OF TABLES

Page

## LIST OF FIGURES

Page

## LIST OF ABBREVIATIONS

| | |
|---|---|
| ACR | American college of radiology |
| ADC | Apparent diffusion coefficient |
| CSF | Cerebrospinal fluid |
| cGM | Cortical gray matter |
| CT | Computed tomography |
| dGM | Deep gray matter |
| DICOM | Digital Imaging and Communications in Medicine |
| DTI | Diffusion tensor imaging |
| DE-TSE | Dual-echo turbo spin-echo |
| DF-FSE | Dual-echo fast spin echo |
| ELGANs | Extremely Low Gestation Age Newborns |
| E42 | Embryonic day 42 |
| ETL | Echo train length |
| FA | Fractional anisotropy |

| | |
|---|---|
| FE | Frequency encoding |
| FSE | Fast spin echo |
| GM | Gray matter |
| ICM | Intracranial matter |
| IR | Inversion recovery |
| LVR | Lateral ventricular ratio |
| MRI | Magnetic resonance imaging |
| mL | Milliliter |
| mm | Millimeter |
| ms | Millisecond |
| NEX | Number of excitation |
| NIH | National institute of health |
| OPCs | Oligodendrocyte progenitor cells |
| PD | Proton density |
| PE | Phase encoding |
| QI | Quantitative Imaging |

| | |
|---|---|
| qMRI | Quantitative MR Imaging |
| ROI | Region of interest |
| T1 | T1 relaxation time |
| T2 | T2 relaxation time |
| TE | Echo time |
| TEeff | Effective echo time |
| TI | Inversion time |
| TR | Repetition time |
| WM | White matter |

# INTRODUCTION

Extremely low gestation age newborns (ELGANs) are defined as infants born before the 28th week after gestation[2]. ELGAN children can have immature function of organs at birth and are at high risk of developmental dysfunction in their life if survive. With advances in new technologies for perinatal and neonatal care, the survival rates for ELGANs have increased dramatically in the past decades. As a result, long-term neurodevelopment problems in ELGANs become a major health issue. Recent studies revealed that ELGAN children had an increased risk for neurodevelopment difficulties in their childhood[2-6]; with 11% of ELGANs in their childhood had cerebral palsy, 11% had microcephaly, 4.5% had macrocephaly, and up to 40% displayed motor deficits [4,5,7]. The incidence of cognitive deficits is even higher, with 30 to 60% of ELGAN children experiencing cognitive impairments, as well as social and emotional difficulties in their childhood[8,9]. These findings indicate that the brain damages in ELGAN children vary with individuals; this variation may reflect important antecedent pathological processes that contribute to brain injury.

Indeed, the functional brain impairments are closely related to the structural brain abnormalities in ELGAN children: two major structural brain abnormalities were observed in ELGAN children at age of 2 years: microcephaly and ventriculomegaly[6]. Microcephaly, defined by a head circumference more than two standard deviations below the external mean at age, is an indicator of reduced brain volume and is associated with severe motor and cognitive impairments[5]. The increased prevalence of microcephaly in

childhood of ELGANs might result from brain damage or diminished brain growth associated with extreme prematurity[2]. Ventriculomegaly, defined by a lateral ventricular ratio (LVR) of greater than 0.32, is common at birth, even in neonates without overt hydrocephalus. Ventriculomegaly is an indicator of brain white matter injury, and are strongly associated with delayed mental and psychomotor development[3,11]. Ventriculomegaly might result from impairment of cerebrospinal fluid (CSF) flow or absorption, or due to diffuse white matter (WM) damage resulting in diminished white matter volume. In addition, when white matter in the brain is damaged, degeneration of the neuron can occur proximally, leading to cortical thinning and microcephaly[12]. Therefore, identifying the relationship of the volumetric changes among gray matter (GM), WM, and CSF is important for understanding the pathological process involved in brain damages of ELGANs. Ventriculomegaly is a leading cause for macrocephaly and occurs in approximately 25% of infants born less than 32 weeks of gestation[12]. However, quantitative determination of the progress of hydrocephalic state in childhood of ELGANs is not readily available in the scientific literature. The impact of hydrocephalus and/or ventriculomegaly on long-term brain development need be addressed by advanced imaging techniques.

In previous ELGANs studies, researchers used ultrasound to detect brain damages and used ventriculomegaly, echodensity, and echolucency as ultrasound biomarkers of white matter damage[3,11]. However, because of its low sensitivity and high inter-observer variability, ultrasound measurement of the brain is less reliable and unable to provide

brain damage information in detail[11]. Volumetric measurement of brain abnormalities to specific tissues or structures is important for understanding the underlying pathogenesis of damages. Magnetic resonance imaging (MRI) studies are much more sensitive than ultrasound in detecting brain development abnormalities in children[13,14]. In particular, quantitative MRI can generate volumetric measurements of cerebral GM and WM development[12,15], which can delineate the characteristics of brain development abnormalities in ELGAN children.

Numerous MRI studies on the structural sequelae of preterm children have emerged in recent decade: these studies reveal that preterm neonates have lower GM and WM volumes at term-equivalent age when compared with term controls of the same age[16-18], and studies of school-aged prematurely born children suggest regional vulnerability in the developing preterm brain[15]. In contrast, MRI studies of preterm subjects at young adult ages fail to document differences in total brain or regional volumes when preterm subjects are compared with either control subjects or their adult-aged siblings[19,20]. Longitudinal volumetric MRI studies of brain show that WM increases while GM decreases at ages from 8 to 12 years for both preterm and full term children, but both the regressive GM changes and increases in WM volumes are significantly less robust in preterm subjects when compared with term controls[21]. The impaired dynamic changes in GM regression and WM growth during this period may have fundamental impact on volumetric changes in brain tissue and in cerebral CSF. However, the brain volumes and the cerebral CSF volumes of ELGAN children at this age period remain

largely unexplored. In this study, we exploited recent advances in MRI data acquisition and post-acquisition processing techniques to measure quantitatively the brain volumes and cerebral CSF volumes of 82 ELGAN children at ages of 9 to 10 years. We hypothesize that ELGAN children at these ages have abnormal GM, WM, and cerebral CSF volumes, even though the total intracranial matter (ICM) volume tends to be normal. To test our hypothesis, we measure the volumetric distribution of total brain (GM + WM), cerebral GM, WM, and CSF, and further analyze the relationships among total brain volume, cerebral GM volume, WM volume, and CSF volume. Our results are compared to brain volumes in population-based normative samples, which are published by the NIH MRI Study of Normal Brain Department [1].

## BACKGROUND

### *1. HUMAN BRAIN COMPOSITION*

The human brain is composed of hundreds of billions of neurons and neuron fibers. Each neuron connects with each other via neuron fibers to build up the information processing systems that are responsible for all of our thoughts, sensations, feelings and actions. The neuron connection site between two neurons is called a synapse. The mature human brain has a characteristic pattern of folds and ridges known as sulci and gyri respectively. The cortex and the subcortical nuclei are called "gray matter" because they contain the cell bodies of neurons and are gray in appearance. Neuron fibers are made of axons and dendrites that extend from cell bodies of the individual neurons.

Dendrites are arrays of short fibers that look like the branches of a tree; they extend only a short distance away from the neuron cell body. Axons are long connecting fibers that extend over long distances and make connections with other neurons, often at the dendrites. Axons are responsible for transmission of electrochemical signals to neurons located in distant locations. Bundles of individual axons from many different neurons within one region of the brain form fiber tracts that make connections with groups of neurons in other regions of the brain forming the information processing networks. Axons wrapped in myelin makes the transmission of electrochemical signals more efficient. Myelin is white in appearance, thus fiber pathways of brain are referred to as "white matter". At the center of the brain are a series of interconnected cavities that form the ventricular system of the brain. The ventricular system is filled with cerebral spinal fluid (CSF) that is recycled several times per day. The ventricular system has a number of important functions including cushioning and protection of the brain, removal of waste material, and transport of hormones and other substances[22].

## *2. BASIC PROCESS OF HUMAN BRAIN DEVELOPMENT*

1) Neuron progenitor cell proliferation: From the end of gastrulation through approximately embryonic day 42 (E42) in humans, the population of neural progenitor cells divides by a mode known as "symmetrical" cell division, which rapidly increases the size of the neural progenitor pool. Beginning on E42, the mode of cell division begins to shift from symmetrical to asymmetrical. During asymmetrical cell division, one neural progenitor cell produces one neural progenitor and one neuron[23]. The new progenitor cell

remains in the proliferative zone and continues to divide, while the postmitotic neuron leaves the proliferative zone to take its place in the developing neocortex. In humans, cortical neurogenesis is complete by approximately E108[24].

2) Neuron differentiation: The different layers of cortex contain different types of neurons. In early corticogenesis, neural progenitor cells are capable of producing any neuron type, but with development they become more and more restricted in the types of neurons they can produce[25,26]. Specific signaling from the growing tissue determines the type of neuron being produced. In order to become integrated into neural networks, the neurons need to develop neuronal processes that allow them to communicate with other neurons. During differentiation, neurons start to develop axons and dendrites that allow them to form communication network with other neurons.

3) Synaptogenesis: Once the axon has reached its target cell's dendrites, synapses are formed with the target cell. Synapses allow for the transmission of electrochemical information, which is the essential means of communication in the brain. During synaptogenesis, the cells of the transient subplate layer of the developing brain play an essential role in establishing neuron communications. When the neural axons arrive at the developing cortex, they do not immediately make connections with target cortex neurons. Rather, they initially make connections with the neurons of the subplate layer. The subplate connections may serve to guide the axons to positions in their target neurons. Once the communication pathways are complete, the subplate neurons retract their connections, and the cells themselves gradually die off [22].

4) Myelination: Oligodendrocyte progenitor cells (OPCs) play important role in axon myelination. Upon reaching its destination, an OPC begins to differentiate and produce myelin protein for its extending processes. The processes then begin to form membrane wraps around nearby axons. Eventually the oligodendrocyte forms tightly wrapped multi-layered sheaths, from which most of the cytoplasm has been extruded. Neuron myelination dramatically increases the velocity of action potential conduction via neuron axons[22].

### *3. DEVELOPMENT OF THE HUMAN BRAIN AFTER BIRTH*

By the end of the prenatal period, major fiber pathways are complete. After birth, brain continues to develop until late adolescent. The brain increases in size by four-fold during the preschool period, reaching approximately 90% of adult volume by age 6[27-30]. However, structural changes in both the major gray and white matter compartments continue through childhood and adolescence, and these changes in structure parallel changes in functional organization that are reflected in behavior. The fundamental postnatal brain development mainly involves synaptogenesis, synaptic pruning, glial cell proliferation, and myelination.

1) Synaptogenesis and synaptic pruning: During the late prenatal and early postnatal period, brain development involves overproduction of neural processes and synapses. The brain overproduces neural connections, or synapses. The level of connectivity throughout the developing brain far exceeds that of adults. This period of synaptic overproduction, termed synaptogenesis, is normally followed by a period of

synaptic retraction, or pruning. This exuberant connectivity is gradually pruned back via competitive processes that are influenced by the experience of the organism. Afferent input plays a critical role in selection of elimination of pathways. The synaptic pruning is a process for refinement and integration of brain networks and confers efficiency on brain functioning. These early experience-dependent processes underlie the plasticity and capacity for adaptation that is one of the hallmarks of early brain development [22].

The time course for synaptic blooming and pruning varies enormously by brain region in humans. The peak of synaptic overproduction in the visual and auditory cortex occurs at about the fourth postnatal month, followed by a gradual retraction until to the end of the preschool age, by which time the density of synapses has reached adult levels. In the area of brain that governs speech and language, a similar but somewhat later time course is observed. In the prefrontal cortex, which is responsible for higher cognitive functions, the peak of synaptic overproduction occurs at around one year of age, and then the density of synapses reduces gradually to the adult level at late adolescence[31].

2) Glial cell proliferation and myelination: Proliferation and migration of glial progenitors begin prenatally, and continue for a protracted period as oligodendrocytes and astrocytes differentiate. Oligodendrocyte progenitor cell proliferation is accompanied by a rapid neuron axon myelination, which after birth, gradually slows down until early adulthood. Most of the axon myelination is completed in the first year after birth. Neuron axon longitudinal growth and myelination contribute to the white matter growth and volume of the brain during childhood.

## *4. ELGANS AND THEIR BRAIN DEVELOPMENT PROBLEMS*

Each year in the US, approximately 32,000 infants are born before the 28th week of gestation and more than 70% survive. More than a third of these ELGAN children will have a major disability. Mild and moderate disabilities after 6 years of age are even more prevalent and are poorly predicted by evaluations before the third birthday. Half the surviving ELGANs without major disability will require support for deficits in attention, executive function, language or academic achievement in their school years[2]. ELGAN-1study is the largest epidemiologic study of ELGANs in the US (1506 infants recruited from 14 hospitals). The study prospectively evaluated approximately 90% of the 1206 surviving children at 24 months corrected age[2]. ELGAN-1 was designed to identify neonatal biomarkers (*e.g.*, proteins in the blood, microorganisms in the placenta, and placental histological lesions) and the results demonstrated that early systematic inflammation is associated with increased risk of cerebral white matter damage in the first postnatal months and neurological abnormalities and delayed cognitive functioning at 2 years[32-34].

Often the initiator of perinatal inflammation is a microorganism. In ELGAN-1, a microorganism was recovered from the placenta parenchyma of 79% of children born at 23 weeks because of preterm labor[35]. In addition, placentas that harbored an organism were more likely than others to have histologic evidence of inflammation. Both organism recovery and histologic inflammation were associated with elevated concentrations of inflammation-related proteins in the newborn's blood. The concentrations of

inflammation-related proteins were also elevated in the cerebrospinal fluid of preterm newborns that develop MRI-documented white matter damage. Infants with the fetal inflammatory response are at increased risk of ventriculomegaly (enlargement of the lateral ventricles of the brain in children, an indicator of reduced brain volume) [34,36-38].

The very processes that lead to preterm delivery, including inflammation and infection, also damage the brain. At basal levels, cytokines have an essential role in normal neuronal and synaptic development. Inflammation not only contributes to preterm brain damage and its consequences, it can also impair processes associated with brain function recovery and plasticity[39].

Elevated concentrations of inflammation-associated proteins might be secondary to the brain damage. Indeed, this can occur in humans and animals following stroke and brain trauma. However, anti-inflammatory therapies given after the first manifestations of the brain damage reduce the final amount of damage. These findings suggest that even if the systemic inflammatory response follows the brain damage, it probably contributes to what is identified as the second wave of damage[40].

Elgan-2 study builds on the results of ELGAN-1. In evaluating the contribution of perinatal inflammation to school-age outcomes, researchers expect to provide a rationale for preventive and therapeutic intervention trials, as well as an ability to identify those at highest risk as targets for clinical trials. Since an inflammatory stimulus alters the expression of more than a thousand genes, it is unlikely that a single protein will be identified as an effective target for prevention or treatment of brain damage. Part of the

ELGAN-2 study is to test the hypothesis that reduced MRI brain volume of white matter, superficial, and deep gray matter in these same three compartments predict neurocognitive impairments, neurobehavioral disorders, and neurological disorders.

### *2.5 QUANTITATIVE MRI (qMRI) MEASUREMENT OF THE HUMAN BRAIN*

MRI is a safe technique for use in children and becomes a widely used tool for brain development study. Tissue changes caused by a range of brain disease have been correlated with qMRI measures (Tofts P. Quantitative MRI of the brain: measuring changes caused by disease: John Wiley & Sons Inc, 2003). The generation of qMRI parameter maps is currently possible with standard clinical MRI scanners using an image acquisition protocol that is easily tolerated by children. This permit researchers to generate imaging information that are used to assess both qualitative brain tissue integrity (abnormal signal) and quantitative measures of brain grey and white matter (hydration level, anisotropy and volumetrics).

Unlike traditional MRI pixel values, which are devoid of scientific units and are non-standardized, qMRI parameters represent physico-biologic tissue quantities, which bear standard units of measurement –*e.g.* seconds, g/cm$^3$-- and are therefore well-defined scientific quantities. For this reason, qMRI pixel values are a more precise and direct reflection of tissue structure than traditional qualitative pixel values. As a result, imaging information derived with qMRI has a high degree of consistency, which can be standardized among different scanner platforms with minimal inter- and intra-site

variance. Consequently, qMRI is becoming the preferred technique for multi-site, multi-platform studies.

Quantitative Imaging (QI) is gradually gaining acceptance in the scientific community particularly for studying the brain. The main objective of QI is to elevate each pixel value of an image into a scientific grade measurement that can be interpreted independently of other pixels in the data set. This permits standardization across imaging platforms, across imaging sessions, and ultimately standardized among different patients. The QI concept entails processing images on a pixel-by-pixel basis to remove the experimental information that is unrelated to the patient and is therefore superfluous -- such as the scanner settings and the detection sensitivity factors--, and to retain the pure physical content of the measurement as it relates to the tissue(s) that a pixel represents. In other words, QI processing amounts to purifying the information of each pixel value down to the physical property probed with the radiation experiment of the modality. Images of all modalities can be QI-processed; for example by properly calibrating and intensity correcting the pixel values of an x-ray CT image, a map of the linear attenuation coefficient results that is universally expressed in Hounsfield units, which are related to the local density of electrons. Similarly, gamma-ray images can be QI-processed leading to maps of the radionuclide concentration.

qMRI is unique for several reasons:1) It is multispectral affording many possible qMRI parameters per pixel. 2) These qMRI parameters characterize the states of water and lipids in tissue, and are therefore the most biologically meaningful parameters that

can be determined with any currently established medical imaging modality. 3) All qMRI parameters other than the proton density itself can be mapped using qMRI algorithms based on the principle of differential weighting. This principle, which stems directly from MRI physics, establishes a logical and powerful mathematical paradigm for removing the patient-unrelated experimental contributions of the pixel values.

## MATERIALS AND METHODS

### *1. SUBJECTS AND ETHICS*

One hundred and sixty subjects from an ELGAN-2 sub-cohort have been scanned at various ELGAN-2 clinical sites at age 9 to 10 years: of these, 82 were analyzed at the time allotted for this thesis. All children were born at extremely low gestation age (<28 weeks). The study participants were selected based on the risk levels of brain damages as assessed by their biomarker profile in the first weeks of life during ELGAN-1 studies. Both male and female were enrolled (34 males and 48 females). The average age of the participants is 9.4 years. Study subjects' medical records showed that all participants were given consent by their parents or guardians for the brain scans to be carried on them. Patient's confidentiality was protected following the National Institutes of Health Insurance Portability and Accountability Act guidelines. The institutional review board of Boston University approved the study protocol.

## *2. MR IMAGE ACQUISITION*

All MR imaging were done at 3T (eleven sites) or 1.5T (one site) with scanners from General Electric, Philips Medical Systems, and Siemens using a phased array coil for signal reception and the quadrature body coil for radiofrequency excitation.

The unified protocol for all scanner brands is as follows:

1. Three-plane localizer(<1 minute)
2. High resolution multispectral qMRI

Sequence 1: Low-resolution fast gradient echo

Sequence 2: Dual-echo-FSE (DF-FSE) + IR Dual-echo-FSE (IR-DE-FSE) (see Table 1)

*Table 1: Pulse sequence 2: key scanning parameters*

| | DE-FSE | IR-DE-FSE |
|---|---|---|
| **Geometry** | | |
| Imaging plane | Axial | Axial |
| FE-Acquisition matrix | 256 | 256 |
| FE-Field-of-View (mm) | 240 | 240 |
| PE-percent Field-of-View | 80 | 80 |
| PE percent sampling | 100 | 100 |
| Number of slices | 80 (gap=0) | 80 (gap=0) |
| Acquired voxel | 0.9375 x 0.9375 x 3.00 $mm^3$ | 0.9375 x 0.9375 x 3.00 $mm^3$ |
| Reconstructed voxel | 0.9375 x 0.9375 x 3.00 $mm^3$ | 0.9375 x 0.9375 x 3.00 $mm^3$ |
| **Contrast** | | |
| Echo time (ms) | TEeff1,2 = 7.142 and 100 | TEeff1,2 = 7.142 and 100 |
| Repetition time (ms) | TR=3000 | TR = 3700 |
| Inversion times (ms) | na | TI = 700 |
| Readout(s) | ETL = 16 (8 per echo: centric, linear) | ETL = 16 (8 per echo: centric, linear) |
| b-factors (s $mm^{-2}$) | na | na |
| $\delta$, $\Delta$ (ms) | na | na |
| Fat suppression | no | no |
| **Acquisition** | | |
| Averages (NEX) | 1 | 1 |
| Scan time (min:s) | 4-5 min | 4-5 min |

## *3. SCANNER ACCEPTANCE CRITERIA*

Each scanner-coil-protocol combination was approved from ELGAN-2 imaging scientists before actual MRI scanning of research subjects. Approvals were based on the results of scanning the MRI accreditation phantom of the American College of Radiology with the proposed imaging protocol. Scanning of the ACR phantom (Figure 1)were performed at the start of the project and following any major upgrade of an ELGAN-2 authorized scanner-coil combination. At each institution, only the approved scanner-coil combinations were used. The ACR MRI phantom is a short, hollow cylinder of acrylic plastic closed at both ends. The inside length is 148 mm; the inside diameter is 190 mm. It is filled with a solution of nickel chloride and sodium chloride: 10 mM $NiCl_2$ and 75 mM NaCl. The outside of the phantom has the words "NOSE" and "CHIN" etched into it as an aid to orienting the phantom for scanning, as if it were a head. Inside the phantom are several structures designed to facilitate a variety of tests of scanner performance. For each phantom scan, we generated all qMRI maps and measured with regions-of-interest (ROI) the qMRI parameters proposed for this work. We also performed the following tests: geometric accuracy, high contrast spatial resolution, slice thickness accuracy, image intensity uniformity, and percent-signal ghosting.

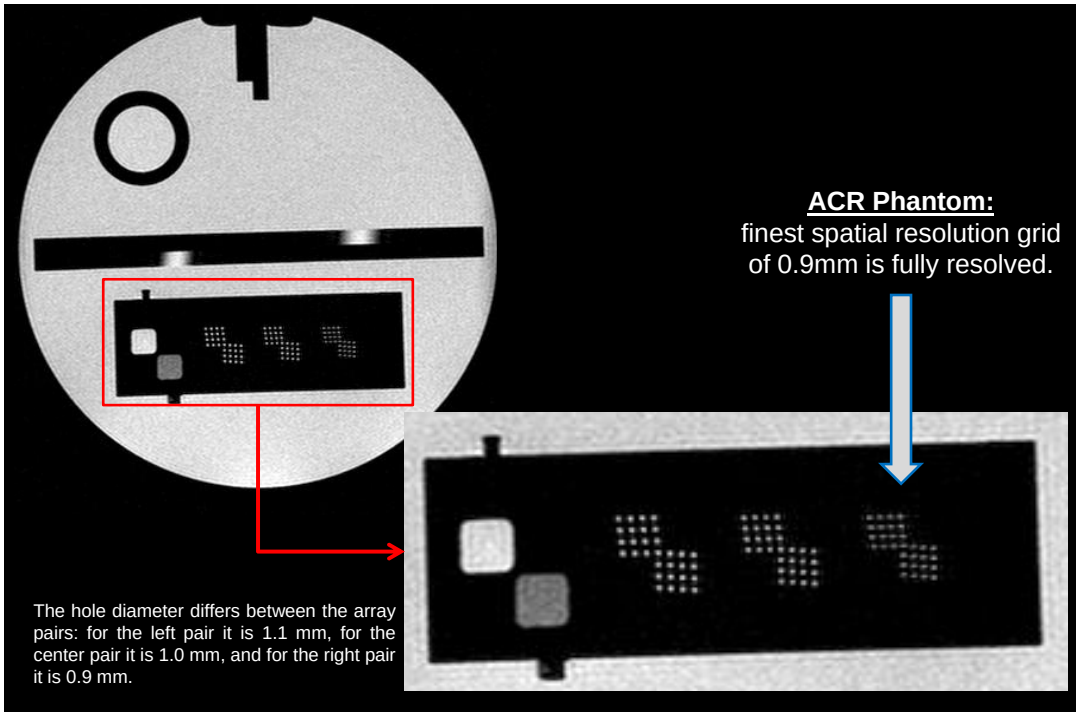


*Figure 1 Example high resolution image of the ACR phantom at the level of the high contrast spatial resolution insert, which is also shown in magnification.*

### *4. IMAGE PREPARATION*

Images generated at all ELGAN-2 sites were sent in DICOM format to the Image Processing Laboratory of the Department of Radiology (BMC) using DVDs, or by electronic means if possible. These DICOM sets were read into an Efilm$^{TM}$ workstation and exported as DICOM files separately for each protocol-pulse sequence. The DICOM headers were removed by Image-J (http://imagej.nih.gov/ij/) using the appropriate batch convertor. In a final preparation step, images were ordered for qMRI processing using an in-house developed algorithm programmed in Mathcad 2001i (PTC, Needham, MA).

### *5. IMAGE PROCESSING: SEGMENTATION*

The segmentation of all tissues in the cranial vault –intracranial matter (ICM) -- was done with a dual-space clustering algorithm[40,41,42], which is applicable to the DE-TSE (FSE) pulse sequence. The operational principle of this dual-clustering algorithm is to interrogate each voxel in the data set as to whether it is contained in both a user-predefined qMRI space subvolume and within a predefined anatomical cluster in anatomic space. With dual-space clustering, segmenting all the intracranial structures — including the CSF — can be accomplished in all slices of the three-dimensional data set with one set of segmentation parameter values. Furthermore, these segmentation parameter values are largely subject-independent. Generated segments were inspected visually for accuracy and this constitutes the bulk of human input time required for segmentation. The user also specifies the intended segmentation side relative to specified bisecting plane.

As illustrated in Figure 2, the whole ICM segment were further divided into the right and left ICMs and then into two subsegments each, (four subsegments): specifically, a cerebral subsegment, an approximate cerebella subsegment. Each bilateral cerebral and cerebellar segment were subsegmented into white matter (WM), deep gray matter (dGM), and cortical gray matter (cGM), and cerebrospinal fluid (CSF) totaling 16 (8 left and 8 right) primary tissue segments. In a final segmentation step, the bilateral cerebral primary tissue segments were divided into anterior and posterior segments, thus totaling 24 (12 left and 12 right) primary tissue segments.

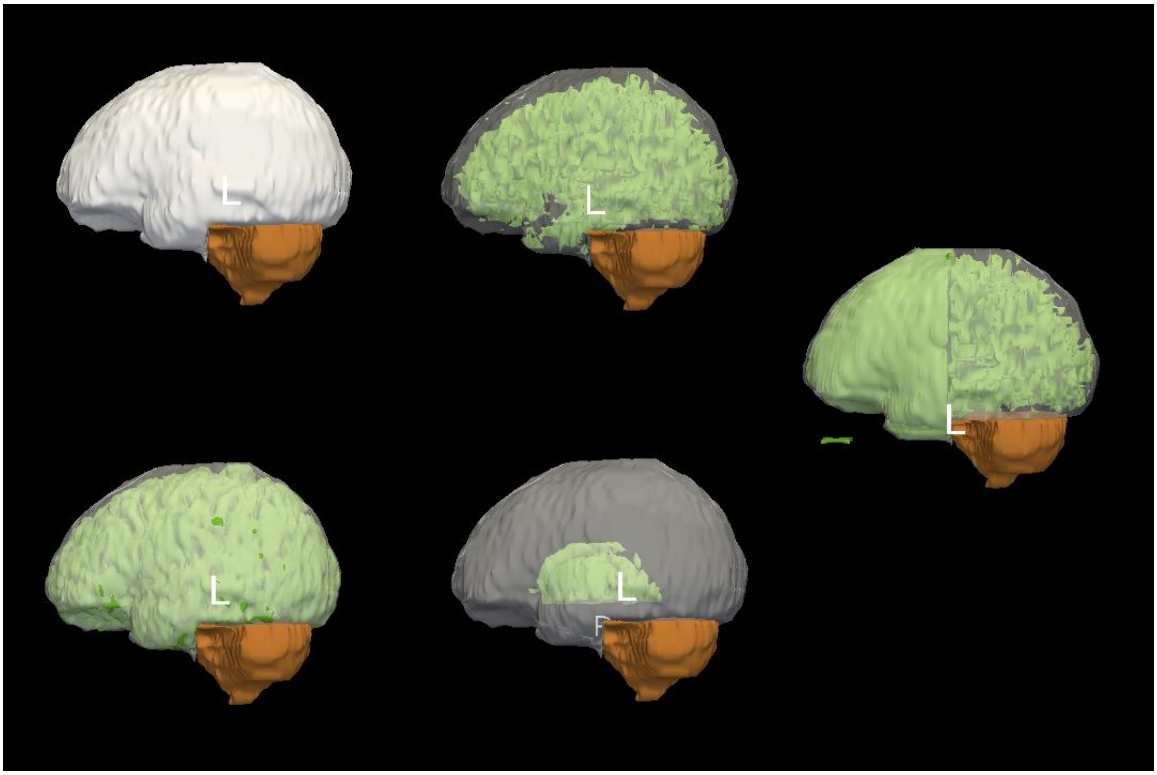


*Figure 2. Proposed segmentation schemes as applied to the left brain: primary segmentation of the cerebral and cerebellar segments (top left). Left cerebrum is subsegmented into WM (top center), dGM (bottom center), and cGM (bottom left). In the final segmentation step the anterior cerebral segments are separated for the posterior ones (middle right).*

## *6. MULTI-SUBJECT ANALYSIS*

For each of the primary tissue type segments, the histograms of all subjects were stored in a single Excel ™ file that is structured as follows: one worksheet per qMRI parameter.

Each of the five Excel files serve as input to an already developed program written in Mathcad that performs gaussian deconvolution on the stored histograms. It generates as output the volumetric and spectral characteristics of each resolved histogram per tissue type (WM, dGM, dGM, and CSF). This histogram analysis process is illustrated in Figure 3 below and has been used[43-45]in our laboratory for processing retrospectively a very large series of isotropic-diffusion (ADC) data.

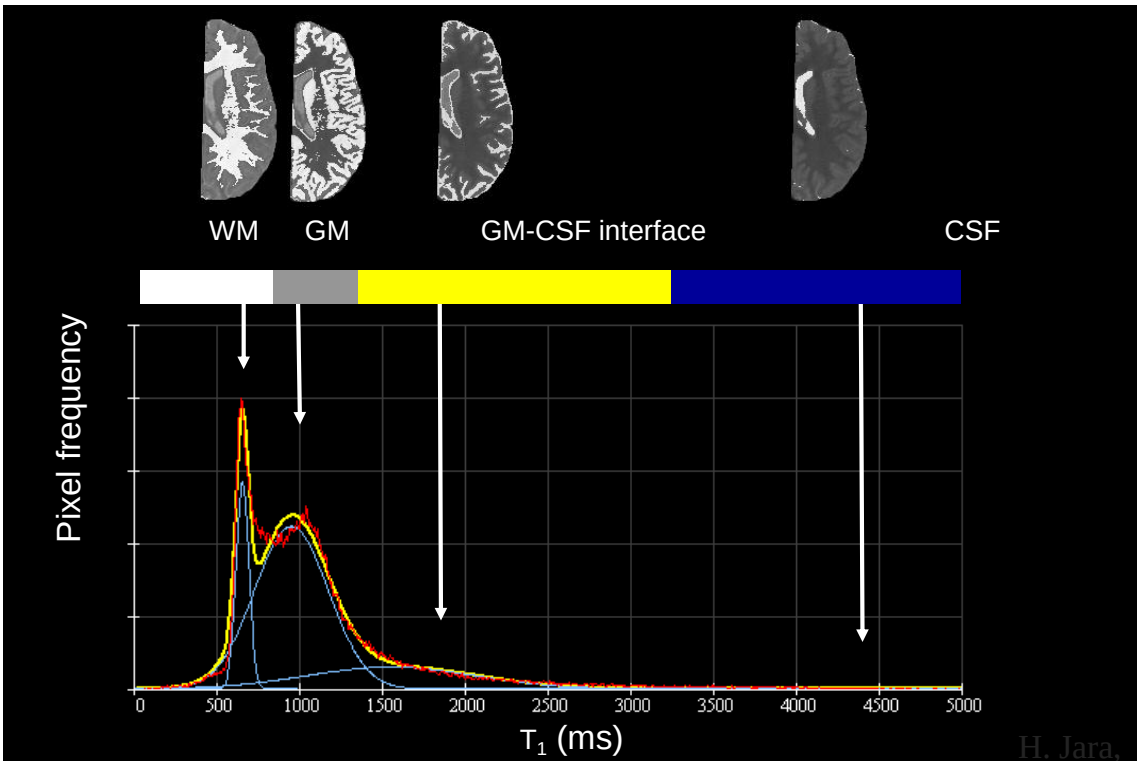


*Figure 3. Classification of T1 spectral features. The four discernable T1 spectral features and their associations with ICM tissue classes (WM, GM, GM–CSF interface and CSF) are shown for one slice of the left brain (27-year-old female). Analogous results are obtained for all slices. Note that tissues classified as GM–CSF interface appear as a discernable spectral feature. Also shown are the individual WM, GM and GM–CSF tissue classes' single-gaussian curves as derived with the three-gaussian fitting algorithm: red and yellow curves are the experimental and the fitted T1 histograms, respectively.*

## *7. STATISTICAL ANALYSIS*

Initial descriptive statistics by brain tissue class and sex were generated based on native, unadjusted brain volume measurements. Total brain volume was defined as the sum of whole brain GM and whole brain WM volume, including the cerebrum, cerebellum, and brainstem (ending at the foramen magnum). Total ICM volume is the sum of total brain and total cerebral CSF volume. Distribution analysis of the total brain volume, GM volume, WM volume, and CSF volume was performed in Microsoft Excel using Data Analysis ToolPak. Correlation analysis between specific brain tissue volumes (Total ICM, total brain, GM, WM) and CSF volume was conducted in Microsoft Excel using the function of statistic tool. Correlation coefficients (r) are given with *p* values (<0.05) to accept or reject significant correlations of brain tissue volumes and CSF volume.

Since the published specific brain volumes of the full term children were presented separately by gender, we calculate the mean volumes and standard deviations of combined male and female data using the following formula:

$$Mean(M) = \frac{M1n1 + M2n2}{n1 + n2}$$

where M is the combined mean of male and female; M1 and M2 are the means of male and female respectively; n1 and n2 are numbers of male and female respectively.

$$Standard\ deviation(S)$$

$$= \sqrt{\frac{n_1^2 s_1^2 + n_2^2 s_2^2 - n_2 s_1^2 - n_2 s_2^2 - n_1 s_1^2 - n_1 s_2^2 + n_2 n_1 s_1^2 + n_2 n_1 s_2^2 + n_1 n_2 (M1 - M2)^2}{(n1 + n2 - 1)(n1 + n2)}}$$

where S is the combined standard deviation of male and female; M1 and M2 are the means of male and female respectively; $n_1$ and $n_2$ are numbers of male and female respectively; $s_1$ and $s_2$ are standard deviations of male and female respectively.

The normalization of mean volumes of the brain tissues by gender is calculated according to the following formula:

$$Normalized\ mean(M_x) = \frac{M_{x1}(m_1 + m_2) + M_{x2}(n_1 + n_2)}{m_1 + m_2 + n_1 + n_2}$$

where $M_{x1}$ and $M_{x2}$ are the mean of X (e.g. total brain volume of ELGANs) for male and female respectively; $m_1$ and $m_2$ are the number of male for ELGANs and full term children respectively; $n_1$ and $n_2$ are the number of female for ELGANs and full term children respectively.

Student's t-test was used to test the difference between two independent means using the following formula:

$$t = \frac{M1 - M2}{\sqrt{\frac{(n1-1)S1^2 + (n2-1)S2^2}{n1+n2-2}\left(\frac{1}{n1} + \frac{1}{n1}\right)}}$$

where M1 and M2 are the means for two independent populations; n1 and n2 are are the numbers for population 1 and population 2 respectively; S1 and S2 are standard deviations of the two different means. $p$ value < 0.05 is a significance level.

## RESULTS

### *1. BRAIN VOLUMES*

Volumetric analysis of brain tissue was performed in the 82 ELGAN children at 9 to 10 years of age. As shown in Table 2, the average total brain volume (GM + WM) in mL, including cerebral hemispheres, cerebellum, and brain stem, of ELGAN children is 1157.7 ± 175, which is smaller (<0.00001) than that from published data of normal term children at same ages (1265.5 ± 115)[1]. Brain volume reduction is more evident in males (10.7% smaller volume, p=0.003) than in females (7.3% smaller volume, p=0.0056). However, when subsegmented into individual tissue types (*i.e.* GM and WM), we found that the GM mean volumes were slightly increased by 1% (p=0.3918) and 8.3% (p=0.0061) in male and female respectively; but the WM mean volumes dramatically reduced by 28.4% (p<0.00001) and 32.1% (p<0.00001) for male and female respectively. Cerebral CSF mean volumes increased 66.4% (p=0.0035) in male and 18.9% (p=0.0136) in female. Since male children have larger brain volumes than female in general, we further normalized the mean volumes of total brain, GM, WM, and CSF by gender, and

the normalized mean volumes demonstrated that the ELGAN children had smaller total brain volume with high reduction of WM and slightly enlargement of GM.

*Table 2: Comparison of brain volumes (ml) of ELGAN children with that of normal term children*

| | Region | Male | Female | Total | Mean normalized by |
|---|---|---|---|---|---|
| This study | | (mean±SD, n=34) | (mean±SD, n=48) | (mean±SD, n=82) | sex |
| | GM+WM | 1197.1±160 | 1129.7±182 | 1157.7±175 | 1157.0 |
| | GM | 848.1±132 | 830.6±130 | 837.9±130 | 837.7 |
| | WM | 349.0±78 | 299.1±80 | 320±83 | 319.3 |
| | CSF | 169.9±120 | 130.4±72 | 146.8±96 | 146.4 |
| NIH | | (mean±SD, n=21) | (mean±SD, n=34) | (mean±SD, n=55) | |
| | GM+WM | 1340.2±106.1 | 1219.4±103.8 | 1265.5±114.9 | 1268.2 |
| | GM | 839.4±73.8 | 767.1±75.1 | 794.7±81.9 | 796.3 |
| | WM | 487.2±63.3 | 440.7±54.4 | 458.4±63.5 | 459.5 |
| | CSF* | 94.9±29 | 101.5±25 | 99±26 | 98.8 |
| *p* value | GM+WM | 0.0003 | 0.0056 | 0.0000 | NA |
| (This | GM | 0.3918 | 0.0061 | 0.0147 | NA |
| study vs. | WM | 0.0000 | 0.0000 | 0.0000 | NA |
| NIH) | CSF* | 0.0035 | 0.0136 | 0.0004 | NA |

## *2. DISTRIBUTION OF BRAIN TISSUE VOLUMES*

From the above analysis, we found that the brain volume distribution of ELGAN children was much wider than that of normal term children. As shown in Figure 4, the total brain volumes of ELGAN children had a wide range from 400 to 1500 ml. Total of 63% of ELGAN children (74% of males and 50% of females) had brain volumes more

than one standard deviation below the mean brain volume of full term children. Still, 5% of ELGAN children had total brain volumes more than one standard deviation above the mean volume of normal term children (4.8% of males and 5.3% of females).

Cerebral GM volume, including cortical and subcortical GM, also covered a wide range from 350 to 1000 ml. As shown in Figure 5, some of the ELGAN children had larger GM volumes than did normal term children, with 32% of ELGAN children (29% of males and 35% of females) having GM volumes more than one standard deviation above the mean GM volume of normal term children. Others had smaller GM volumes than did normal term children, with 15% of ELGAN children (31% of males and 4.8% of female) having GM volumes more than one standard deviation below the mean of normal term children.

Cerebral WM volumes of ELGAN children ranged from 100 to 500 ml (Figure 6). Unlike the GM, the WM of ELGAN children reduced dramatically when compared to normal term children. There were 90% of ELGAN children (86% of males and 9% of females) having smaller WM volumes, which were more than 1 standard deviation below the mean volume of WM of normal term children. However, none had WM volume larger than 1 standard deviation above the mean of normal term children.

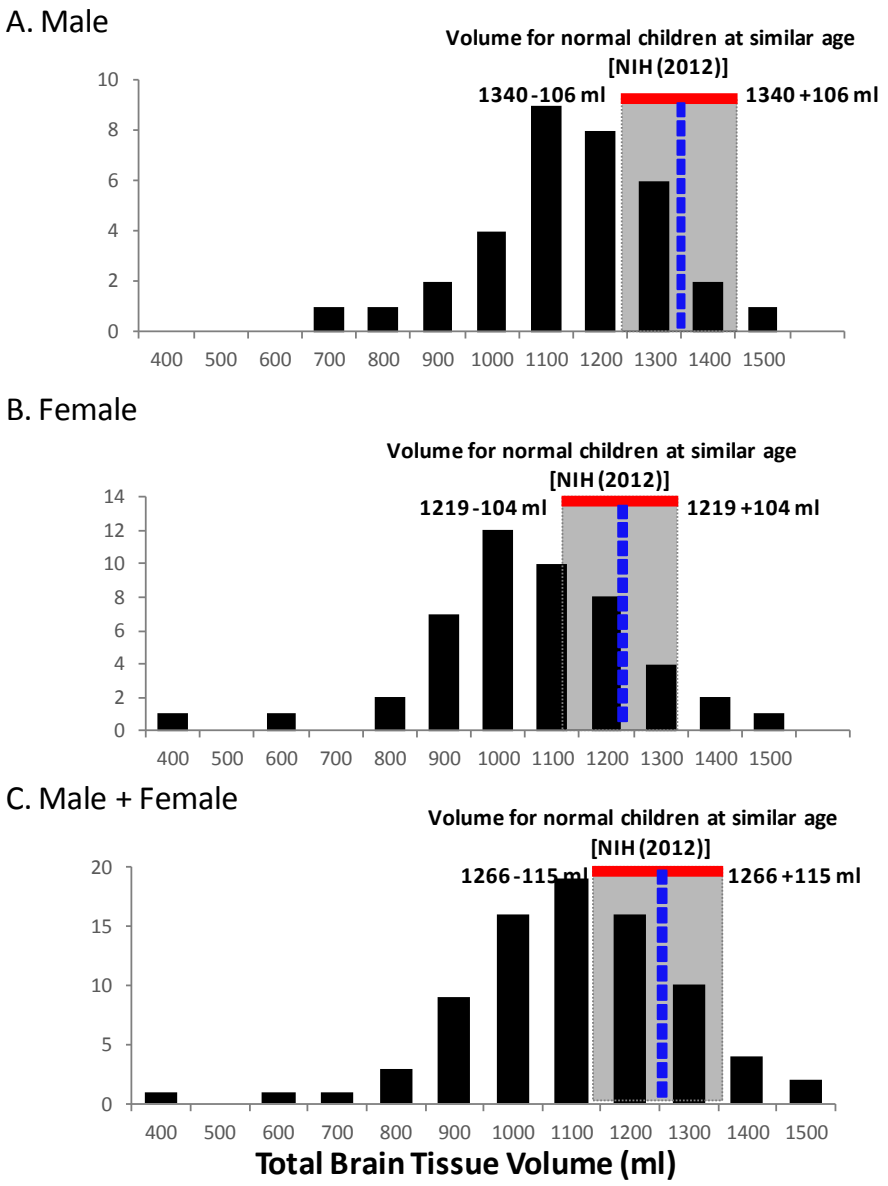


*Figure 4. Total brain tissue volume of ELGAN children shows nearly Gaussian distribution with wide range. The mean total brain volume together with its standard deviation of full-term children at the same age*[1]*is superimposed on the distribution graph. Dotted blue line indicates the mean volume of the full term children; Red line indicates the size of standard deviation.*

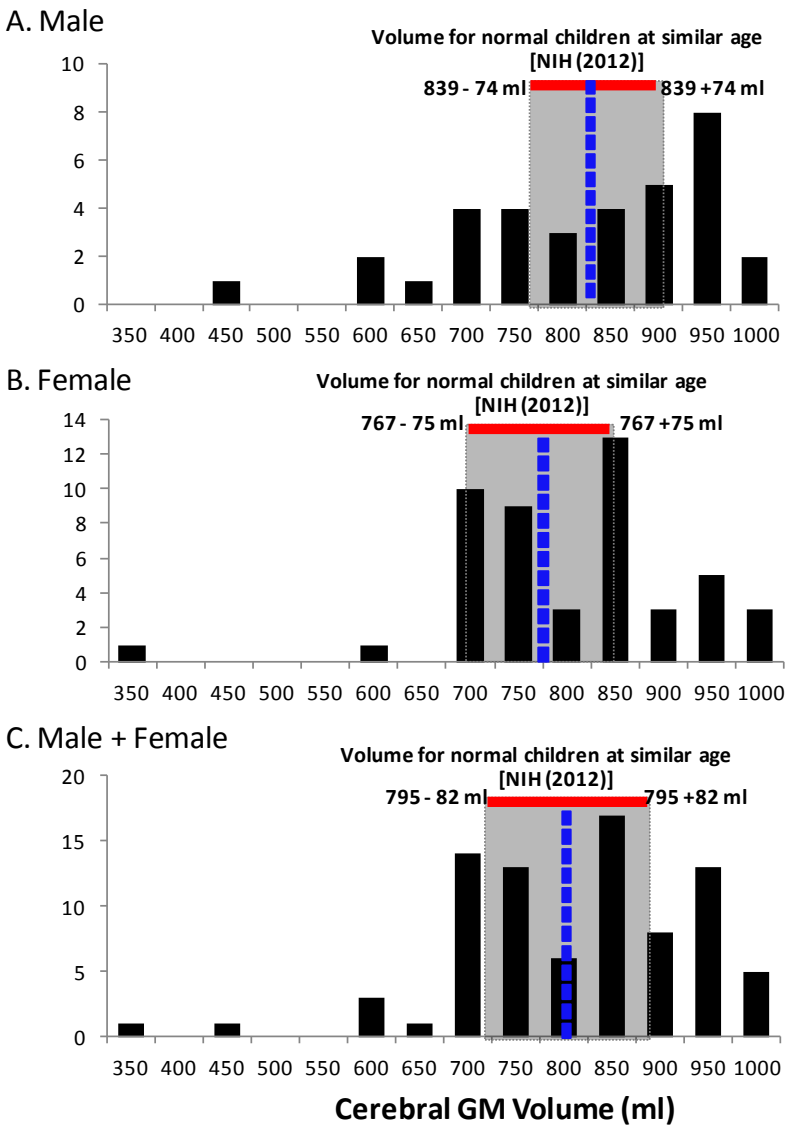


*Figure 5. Total GM volume of ELGAN children shows abnormal distribution with wide range. The mean total GM volume together with its standard deviation of full-term children at the same age* [1] *is superimposed on the distribution graph. Dotted blue line indicates the mean volume of the full term children; Red line indicates the size of standard deviation.*

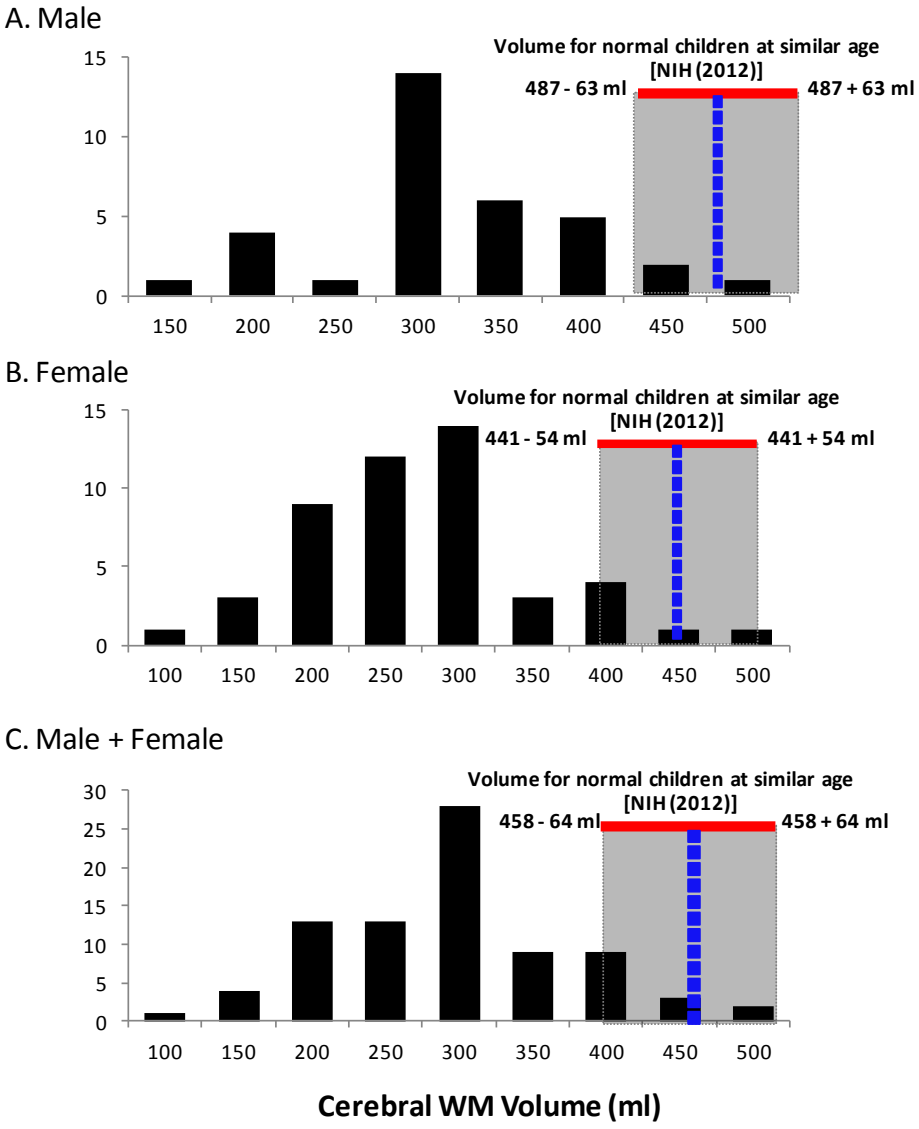


*Figure 6. Total WM volume of ELGAN children shows nearly Gaussian distribution with wide range. The mean total WM volume together with its standard deviation of full-term children at the same age[1]is superimposed on the distribution graph. Dotted blue line indicates the mean volume of the full term children; Red line indicates the size of standard deviation.*

Intracranial CSF volumes, which comprises extra cerebral (including sulcal) and ventricular CSF but excluding cerebellum CSF, had a very large distribution range in ELGAN children as shown in Figure 7. The smallest CSF volume was as low as 25 ml and the largest CSF volume was as high as 600 ml. Most of the ELGAN children had larger CSF volumes than did normal term children. Thirty-eight percent of ELGAN children (52.9% of males and 27.1% for females) had large CSF volumes, which were more than 1 standard deviation above the mean volume of CSF of normal term children. Still there were 15.9% of ELGAN children (8.8% of males and 20.8% of females) having CSF volumes more than 1 standard deviation below the mean CSF volume of normal term children.

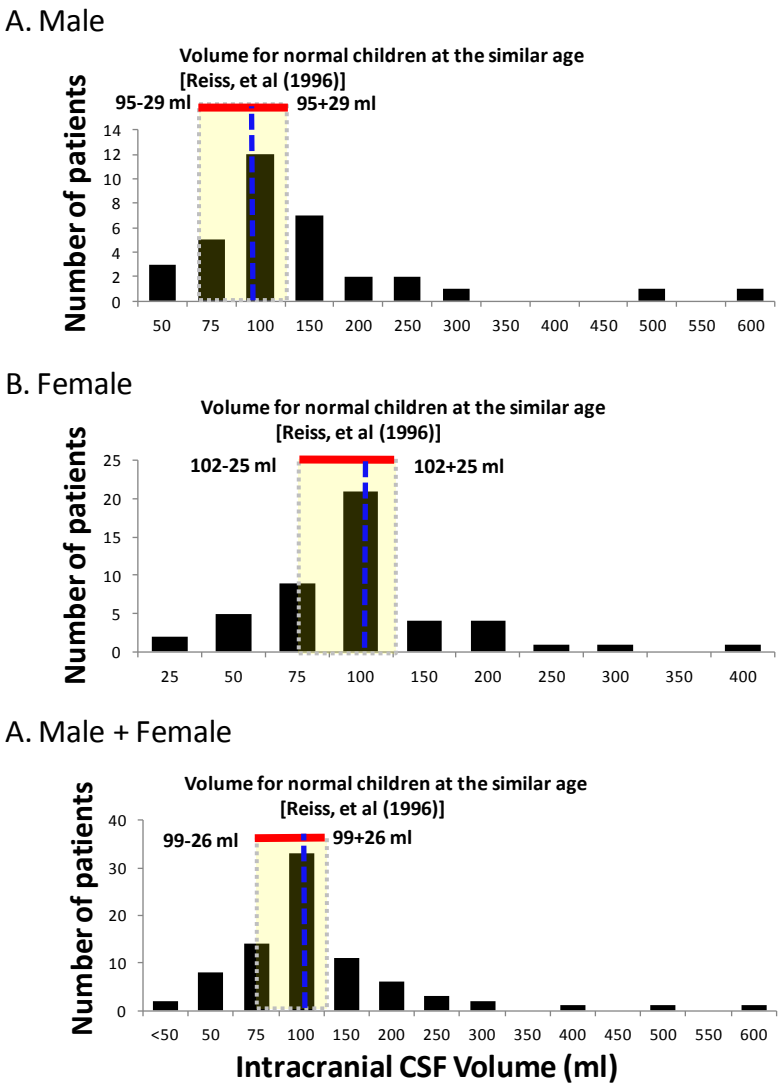


*Figure 7. Total brain CSF volume of ELGAN children shows skewed distribution with wide range. The mean total brain CSF volume together with its standard deviation of full-term children at the same age[27] is superimposed on the distribution graph. Dotted blue line indicates the mean volume of the full term children; Red line indicates the size of standard deviation.*

### *3. CORRELATION ANALYSIS OF BRAIN TISSUE AND INTRACRANIAL CSF*

To address the relationship of intracranial CSF volume with total ICM volume, total brain volume, cerebral GM volume, and WM volume, we analyzed the CSF-related changes of those brain volumes by correlation analysis.

Total ICM volumes of ELGAN children were positively correlated with intracranial CSF volumes, both in male ($r = 0.4972$, $p = 0.0014$) and in female ($r = 0.3233$, $p = 0.0125$), while total brain volumes were negatively correlated with CSF volumes both in male ($r = -0.2998$, $p = 0.0424$) and in female($r = -0.2279$, $p = 0.0596$) (Figure 8).

Cerebral GM of either male or female showed a negative correlation with intracranial CSF both in absolute GM volume (male: $r = -0.4489$, $p = 0.0039$; female: $r = 0.3769$, $p = 0.0041$) and in relative GM volume (GM/ICM ratio) (male: $r = -0.8675$, $p = 0.0000$; female: $r = 0.8350$, $p = 0.0000$). (see Figure 9)

There was no correlation between total cerebral WM volumes and intracranial CSF volumes, either in absolute or in relative volumes (Figure 10).

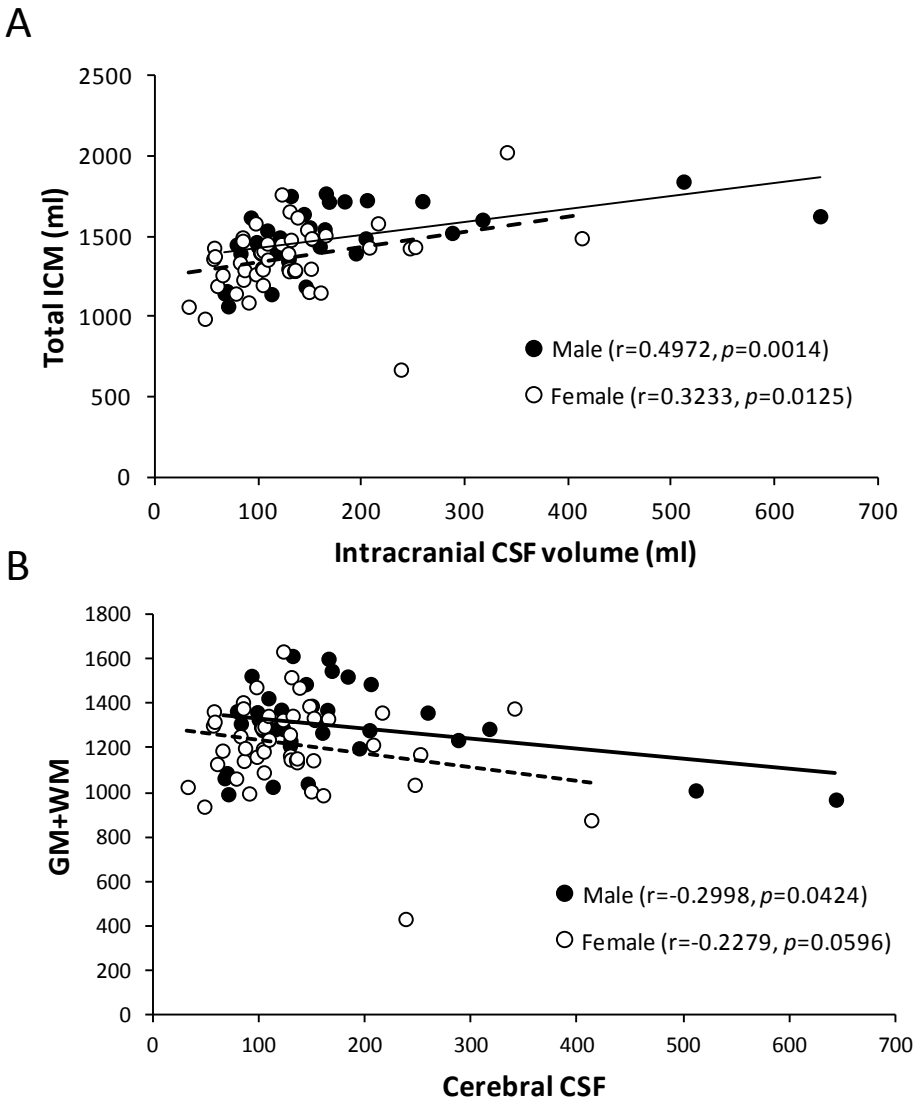


*Figure 8. (A) The scatterplot shows the absolute volume of total ICM changing with cerebral CSF volume in all ELGAN children. Total ICM volume is positively correlated with cerebral CSF volume both in male and in female. (B) The scatterplot shows the absolute volume of total brain tissue (GM+WM) changing with cerebral CSF volume in all ELGAN children. Total brain volume is negatively correlated with cerebral CSF volume in both male and female.*

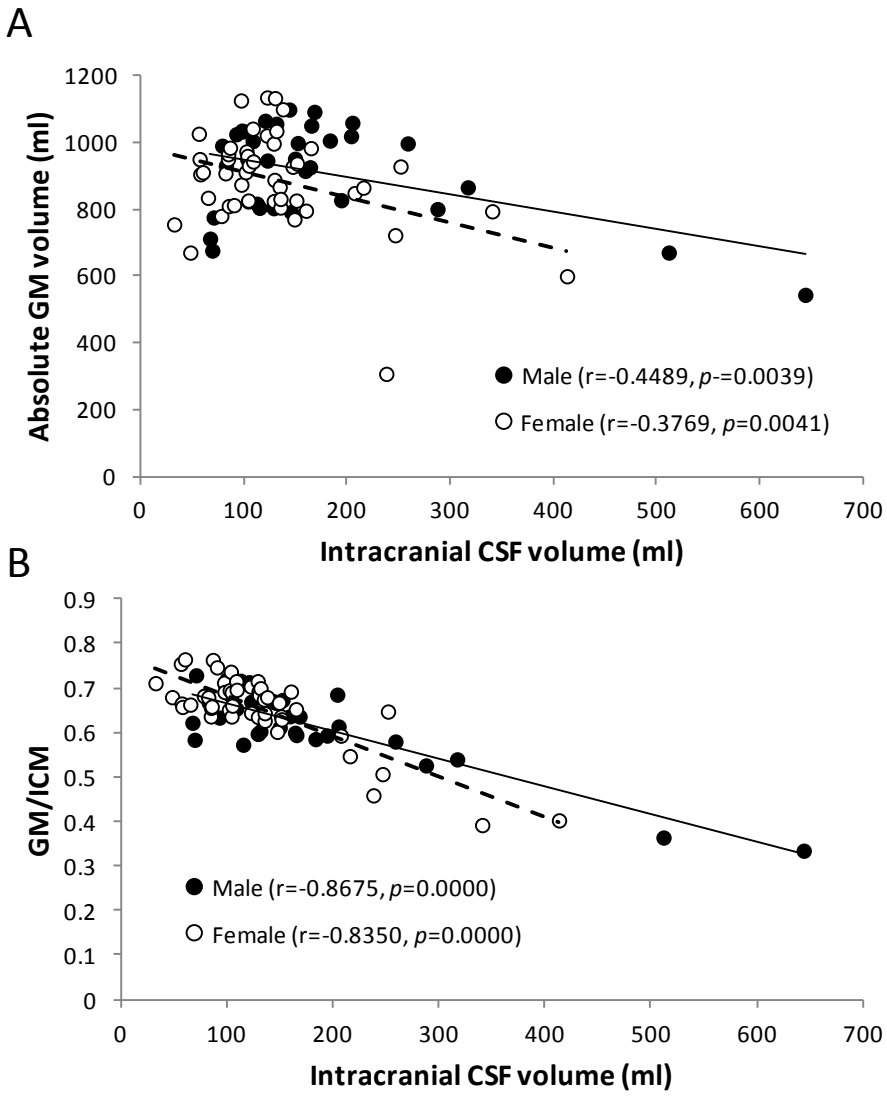


*Figure 9. (A) The scatterplot shows the absolute volume of total GM changing with cerebral CSF volume in all ELGAN children. Total GM volume is negatively correlated with cerebral CSF volume in both male and female. (B) The scatterplot shows the relative volume of total brain GM as a percentage of ICM volume in all ELGAN children. The relative brain volume is negatively correlated with cerebral CSF volume in both male and female.*

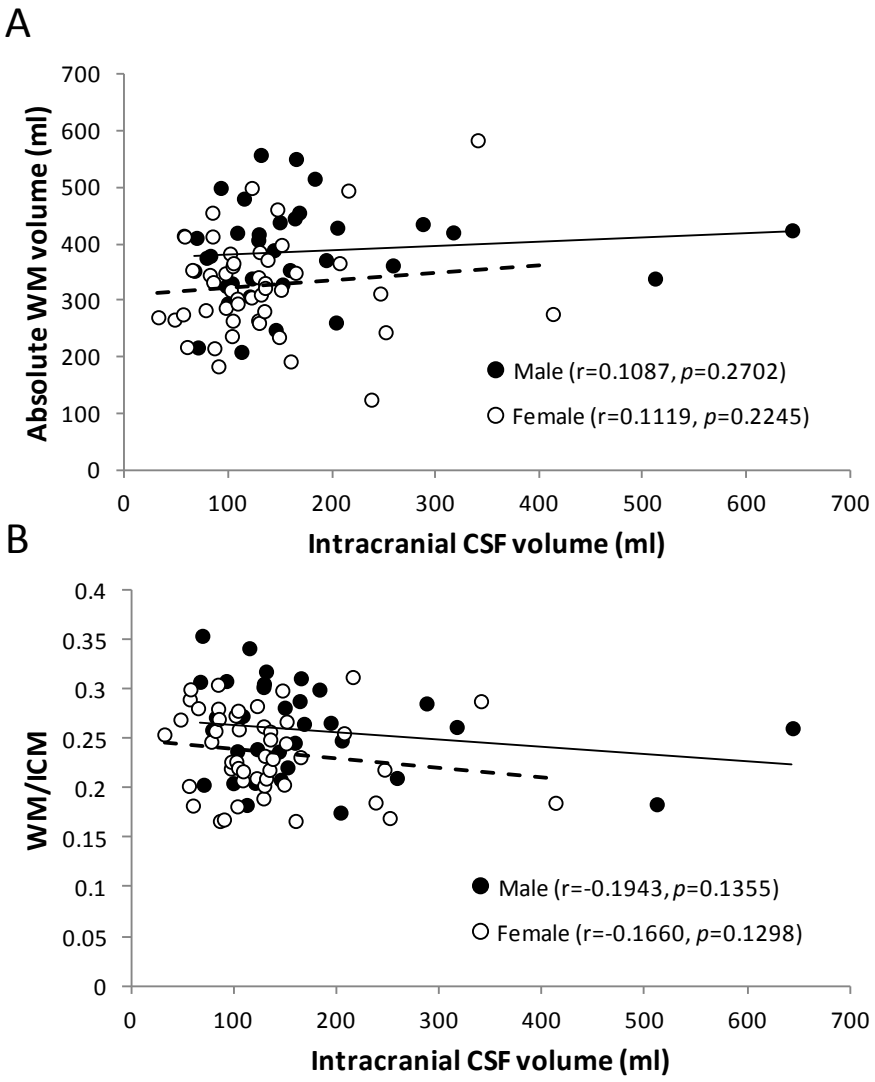


*Figure 10. (A) The scatterplot shows the absolute volume of total WM changing with cerebral CSF volume in all ELGAN children. Total WM volume has no significant correlation with cerebral CSF volume in both male and female. (B) The scatterplot shows the relative volume of total WM as a percentage of ICM volume in all ELGAN children. The relative WM volume has no significant correlation with cerebral CSF volume in both male and female.*

## DISCUSSION

In this study, we measured the whole brain GM, WM, and CSF volumes in a sub-group of eighty-two ELGAN children using segmentation algorithms based on quantitative MRI. Our results revealed a mean reduction of total brain volume and WM volume, but an increase in CSF volume. GM volumes either increased or decreased, but the average of the volume was slightly increased. The brain volumes distributions are wide. A large number of subjects had significant reduction of total brain volumes, while a small number of subjects had enlargement of total brain volumes at the age of 9 to 10 years. Decreased WM volumes in all children and GM volumes in some children are the major causes of small brain volumes; but increased GM and CSF volumes are the primary contributors to larger ICM volumes. Both total brain volume and cerebral GM volume had negative correlations with CSF volume, while WM volume had no significant correlation with CSF volume. This indicates that cerebral CSF volume abnormalities may have an effect on cerebral GM, but not on WM development.

Both reduction and enlargement of cerebral GM volumes found in ELGAN children may indicate that various etiologies during perinatal period and childhood give rise to different types of damages of premature brains. The main etiological pathway relates to brain damage due to inflammation is mediated by cytokines. Cytokines in the brain not only act as inflammatory mediators, but also act as physiologic and trophic factors to stimulate neuron proliferation, differentiation, migration, and synaptogenesis.

The pathological process mediated by inflammation might result in over production of neuron and glial cells, and eventually enlarged GM volume.

Brain volume reduction and/or GM loss is consistent with the results of previous studies on preterm infants or in preterm children less than 2 years old[15, 49-53]. Our finding confirmed that GM reduction still existed in many ELGAN children at school age. Although total brain volume and/or total GM enlargement in preterm children was rarely reported previously, regional brain volume enlargement in the occipital and temporal areas was found in preterm children at the age of eight years[15]. The total brain volume and/or total GM enlargement in some ELGAN children might indicate an impairment of important brain development processing, such as synaptic pruning, happened specifically at this age period. In fact, the ongoing process of pruning and cell death of neurons and glial cells resulted in a rapid GM regression in normal children at this age period[54, 55]. Longitudinal studies suggested a childhood increase in GM volume followed by a decrease from pre-teenage to adulthood[54], but the GM volume reduction rate was significantly lower in preterm children than in normal controls between the age of 8 and 12 years[21]. These findings provide us a reasonable explanation that the increased GM volumes in some of our studied subjects might due to a decrease in the normal occurrence of synaptic pruning and /or an increase in glial cells expansion resulting from chronic inflammation.

Unlike GM changes, WM volume reduction in ELGAN children was uniformly seen in both male and female subjects, which is consistent with previous studies of

preterm infants and young children[21,53,56]. WM reduction is the most prominent change in preterm children at all ages until early adult[30,54,55]. The causes of WM reduction include primary WM damage and impaired ongoing axon myelination. Ventricular hemorrhage and ischemia are the most common causes to WM injury encountered in the human premature infants[57,58]. The effect of these insults in premature infants on subsequent myelination has been determined by qMRI assessment[12]. The myelination impairment may exist throughout the postnatal brain development in preterm children because WM volume increases linearly with age in both full term and preterm children, but preterm children had a much lower WM increase rate than did full term children at all ages[21,54,55,59] . Further study of neuron fiber myelination of ELGAN children from school age to adulthood is required to address this issue.

Studies of preterm infants and young children revealed an increase in cerebral CSF volume[50,51,60]. Here we found that most of the ELGAN children had increased CSF volume while some of them had decreased CSF volume. The alteration of CSF volume can cause changes in composition of CSF. Finely regulation of composition in CSF is vital to brain development and brain health. Brain damage in ELGAN children might impair CSF circulation and adversely affect the neuron growth and functions. Increased cerebral CSF volume in ELGAN children might indicate abnormal ventricular flow and/or defect CSF absorption, while decreased CSF volume might indicate problem of CSF production due to choroid plexus malfunction. The abnormality of CSF might mainly affect GM volume, but not WM volume; because negative correlation between

GM volume and CSF volume was found in ELGAN children while no correlation was found between WM and CSF volumes. Recent studies revealed an important role of CSF in brain cortical development and demonstrated that hydrocephalus inhibited cortical GM growth in animals[261,62]. The cortical thinning of hydrocephalus animals was not due to either altered compression/stretching of the brain or excessive cell death in the cortex, but due to the inhibition of the germinal matrix stem and progenitor cell proliferation in the developing brain by a new protein in the obstructed CSF[61].

There are a number of limitations to the current study. First, given the heterogeneity in brain development of preterm children the sample size in this study is relatively small. This study is also limited by having only preterm subjects while lack of age- and sex-matched normal term controls. Our results were compared to previously published data of normal term children. This comparison is less rigorous and the study should be considered descriptive and exploratory. In addition, the cross-sectional nature of the study prevented us from exploring whether brain volume differences changed across childhood to adolescence. Longitudinal studies of brain development would help clarify the trajectory of GM and WM tissue growth in ELGAN children. Finally, the key question in neuroanatomical MRI studies is what a change in the volume of a brain tissue in a given disorder means. Although gross differences in volumes of brain structures can be quantified, individual cells and cell layers cannot yet be visualized. This means that, although the volume and shape of brain structures may be determined, the underlying cause of any differences cannot.

## CONCLUSION

ELGAN children had mostly smaller brain volumes while some of them displayed larger brain volumes at ages of 9 to 10 years. The reduction of WM was a characteristic change in ELGAN children and contributed to smaller brain volumes. GM volumes either increased or decreased. Larger intracranial CSF volumes were associated with larger intracranial matter (ICM) volume. We summarize some key points as below:

1. Total brain volumes decrease in most ELGAN children, but increase in a small portion of ELGAN children.
2. Males are more vulnerable to decreasing in brain volume than are females.
3. GM volume either increases or decreases in male and female; but males more often display GM reduction, while females more often show increased GM.
4. WM reduction is uniformly seen in both male and female.

The volumetric analysis of the developing brain of an ELGAN-2 subgroup at 9-to-10 years of age using qMRI-based volumetrics provides evidence of persisting brain abnormalities at school age.

## LIST OF JOURNAL ABBREVIATIONS

| | |
|---|---|
| Acta Paediatr | Acta Paediatrica |
| Am Psychol | American Psychologist |
| Ann Neurol | Annals of Neurology |
| Arch Dis Child Fetal Neonatal Ed | Archives of Disease in Childhood. Fetal and Neonatal Edition |
| Biol Neonate | Biology of the Neonate |
| Br J Pharmacol | British Journal of Pharmacology |
| Brain Behav Immun | Brain, Behavior, and Immunity |
| Can J Physiol Pharmacol | Canadian Journal of Physiology and Pharmacology |
| Curr Opin Neurobiol | Current Opinion in Neurobiology |
| Dev Med Child Neurol | Developmental Medicine and Child Neurology |
| Dev Sci | Developmental Science |
| Early Hum Dev | Early Human Development |
| J Am Acad Child Adolesc Psychiatry | Journal of the American Academy of Child and Adolescent Psychiatry |
| J Child Neurol | Journal of Child Neurology |
| J Dev Behav Pediatr | Journal of Developmental and Behavioral Pediatrics |
| J Int Neuropsychol Soc | Journal of the International Neuropsychological Society |
| J Pediatr | Journal of Pediatrics |
| JAMA | JAMA: The Journal of the American Medical Association |

| | |
|---|---|
| Magn Reson Imaging | Magnetic Resonance Imaging |
| Mech Dev | Mechanisms of Development |
| Med Phys | Medical Physics |
| N Engl J Med | New England Journal of Medicine |
| Nat Neurosci | Nature Neuroscience |
| Neuropsychol Rev | Neuropsychology Review |
| Pediatr Neurol | Pediatric Neurology |
| Pediatr Res | Pediatric Research |
| Semin Fetal Neonatal Med | Seminars in Fetal & Neonatal Medicine |
| Surg Neurol | Surgical Neurology |

## LIST OF REFERENCES


1. Brain Development Cooperative Group. Total and regional brain volumes in a population-based normative sample from 4 to 18 years: The NIH study of normal brain development. *Cerebral Cortex*. 2012;22(Oxford University Press):1-12.

2. O'Shea TM, Allred EN, Dammann O, et al. The ELGAN study of the brain and related disorders in extremely low gestational age newborns. *Early Hum Dev*. 2009;85(11):719-725. doi: 10.1016/j.earlhumdev.2009.08.060 [doi].

3. Kuban KC, Allred EN, O'Shea M, et al. An algorithm for identifying and classifying cerebral palsy in young children. *J Pediatr*. 2008;153(4):466-472. doi: 10.1016/j.jpeds.2008.04.013 [doi].

4. Kuban KC, Allred EN, O'Shea TM, et al. Cranial ultrasound lesions in the NICU predict cerebral palsy at age 2 years in children born at extremely low gestational age. *J Child Neurol*. 2009;24(1):63-72. doi: 10.1177/0883073808321048 [doi].

5. Kuban KC, Allred EN, O'Shea TM, et al. Developmental correlates of head circumference at birth and two years in a cohort of extremely low gestational age newborns. *J Pediatr*. 2009;155(3):344-9.e1-3. doi: 10.1016/j.jpeds.2009.04.002 [doi].

6. O'Shea TM, Kuban KC, Allred EN, et al. Neonatal cranial ultrasound lesions and developmental delays at 2 years of age among extremely low gestational age children. *Pediatrics*. 2008;122(3):e662-9. doi: 10.1542/peds.2008-0594 [doi].

7. Holsti L, Grunau RV, Whitfield MF. Developmental coordination disorder in extremely low birth weight children at nine years. *J Dev Behav Pediatr*. 2002;23(1):9-15.

8. Taylor HG, Minich N, Bangert B, Filipek PA, Hack M. Long-term neuropsychological outcomes of very low birth weight: Associations with early risks for periventricular brain insults. *J Int Neuropsychol Soc*. 2004;10(7):987-1004.

9. Laptook AR, O'Shea TM, Shankaran S, Bhaskar B, NICHD Neonatal Network. Adverse neurodevelopmental outcomes among extremely low birth weight infants with a normal head ultrasound: Prevalence and antecedents. *Pediatrics*. 2005;115(3):673-680. doi: 115/3/673 [pii].

10. Bell WO, Arbit E, Fraser RA. One-stage meningomyelocele closure and ventriculoperitoneal shunt placement. *Surg Neurol*. 1987;27(3):233-236.

11. Krishnamoorthy KS, Kuban KC, O'Shea TM, et al. Early cranial ultrasound lesions predict microcephaly at age 2 years in preterm infants. *J Child Neurol*. 2011;26(2):188-194. doi: 10.1177/0883073810377017 [doi].

12. Huppi PS, Warfield S, Kikinis R, et al. Quantitative magnetic resonance imaging of brain development in premature and mature newborns. *Ann Neurol*. 1998;43(2):224-235. doi: 10.1002/ana.410430213 [doi].

13. Mirmiran M, Barnes PD, Keller K, et al. Neonatal brain magnetic resonance imaging before discharge is better than serial cranial ultrasound in predicting cerebral palsy in very low birth weight preterm infants. *Pediatrics*. 2004;114(4):992-998. doi: 114/4/992 [pii].

14. Woodward LJ, Anderson PJ, Austin NC, Howard K, Inder TE. Neonatal MRI to predict neurodevelopmental outcomes in preterm infants. *N Engl J Med*. 2006;355(7):685-694. doi: 355/7/685 [pii].

15. Peterson BS, Vohr B, Staib LH, et al. Regional brain volume abnormalities and long-term cognitive outcome in preterm infants. *JAMA*. 2000;284(15):1939-1947. doi: joc00361 [pii].

16. Counsell SJ, Boardman JP. Differential brain growth in the infant born preterm: Current knowledge and future developments from brain imaging. *Semin Fetal Neonatal Med*. 2005;10(5):403-410. doi: S1744-165X(05)00037-5 [pii].

17. Peterson BS, Anderson AW, Ehrenkranz R, et al. Regional brain volumes and their later neurodevelopmental correlates in term and preterm infants. *Pediatrics*. 2003;111(5 Pt 1):939-948.

18. Srinivasan L, Dutta R, Counsell SJ, et al. Quantification of deep gray matter in preterm infants at term-equivalent age using manual volumetry of 3-tesla magnetic resonance images. *Pediatrics*. 2007;119(4):759-765. doi: 119/4/759 [pii].

19. Allin M, Henderson M, Suckling J, et al. Effects of very low birthweight on brain structure in adulthood. *Dev Med Child Neurol*. 2004;46(1):46-53.

20. Fearon P, O'Connell P, Frangou S, et al. Brain volumes in adult survivors of very low birth weight: A sibling-controlled study. *Pediatrics*. 2004;114(2):367-371. doi: 114/2/367 [pii].

21. Ment LR, Kesler S, Vohr B, et al. Longitudinal brain volume changes in preterm and term control subjects during late childhood and adolescence. *Pediatrics*. 2009;123(2):503-511. doi: 10.1542/peds.2008-0025 [doi].

22. Stiles J, Jernigan TL. The basics of brain development. *Neuropsychol Rev*. 2010;20(4):327-348. doi: 10.1007/s11065-010-9148-4 [doi].

23. Wodarz A, Huttner WB. Asymmetric cell division during neurogenesis in drosophila and vertebrates. *Mech Dev*. 2003;120(11):1297-1309. doi: S0925477303002053 [pii].

24. Clancy B, Darlington RB, Finlay BL. Translating developmental time across mammalian species. *Neuroscience*. 2001;105(1):7-17. doi: S0306-4522(01)00171-3 [pii].

25. Leone DP, Srinivasan K, Chen B, Alcamo E, McConnell SK. The determination of projection neuron identity in the developing cerebral cortex. *Curr Opin Neurobiol*. 2008;18(1):28-35. doi: 10.1016/j.conb.2008.05.006 [doi].

26. Shen Q, Wang Y, Dimos JT, et al. The timing of cortical neurogenesis is encoded within lineages of individual progenitor cells. *Nat Neurosci*. 2006;9(6):743-751. doi: nn1694 [pii].

27. Reiss AL, Abrams MT, Singer HS, Ross JL, Denckla MB. Brain development, gender and IQ in children. A volumetric imaging study. *Brain*. 1996;119 ( Pt 5)(Pt 5):1763-1774.

28. Iwasaki N, Hamano K, Okada Y, et al. Volumetric quantification of brain development using MRI. *Neuroradiology*. 1997;39(12):841-846.

29. Courchesne E, Chisum HJ, Townsend J, et al. Normal brain development and aging: Quantitative analysis at in vivo MR imaging in healthy volunteers. *Radiology*. 2000;216(3):672-682. doi: 10.1148/radiology.216.3.r00au37672 [doi].

30. Lenroot RK, Gogtay N, Greenstein DK, et al. Sexual dimorphism of brain developmental trajectories during childhood and adolescence. *Neuroimage*. 2007;36(4):1065-1073. doi: S1053-8119(07)00234-0 [pii].

31. Thompson RA, Nelson CA. Developmental science and the media. early brain development. *Am Psychol*. 2001;56(1):5-15.

32. Kuban KC, O'Shea TM, Allred EN, et al. Systemic inflammation and cerebral palsy risk in extremely preterm infants. *J Child Neurol*. 2014;29(12):1692-1698. doi: 10.1177/0883073813513335 [doi].

33. Kuban KC, O'Shea TM, Allred EN, et al. The breadth and type of systemic inflammation and the risk of adverse neurological outcomes in extremely low gestation newborns. *Pediatr Neurol*. 2015;52(1):42-48. doi: 10.1016/j.pediatrneurol.2014.10.005 [doi].

34. Leviton A, Allred EN, Dammann O, et al. Systemic inflammation, intraventricular hemorrhage, and white matter injury. *J Child Neurol*. 2013;28(12):1637-1645. doi: 10.1177/0883073812463068 [doi].

35. Leviton A, Allred EN, Kuban KC, et al. Microbiologic and histologic characteristics of the extremely preterm infant's placenta predict white matter damage and later cerebral palsy. the ELGAN study. *Pediatr Res*. 2010;67(1):95-101. doi: 10.1203/PDR.0b013e3181bf5fab [doi].

36. Leviton A, Kuban KC, Allred EN, et al. Early postnatal blood concentrations of inflammation-related proteins and microcephaly two years later in infants born before the 28th post-menstrual week. *Early Hum Dev*. 2011;87(5):325-330. doi: 10.1016/j.earlhumdev.2011.01.043 [doi].

37. Leviton A, Kuban K, O'Shea TM, et al. The relationship between early concentrations of 25 blood proteins and cerebral white matter injury in preterm newborns: The ELGAN study. *J Pediatr*. 2011;158(6):897-903.e1-5. doi: 10.1016/j.jpeds.2010.11.059 [doi].

38. Leviton A, O'Shea TM, Bednarek FJ, et al. Systemic responses of preterm newborns with presumed or documented bacteraemia. *Acta Paediatr*. 2012;101(4):355-359. doi: 10.1111/j.1651-2227.2011.02527.x [doi].

39. O'Shea TM, Shah B, Allred EN, et al. Inflammation-initiating illnesses, inflammation-related proteins, and cognitive impairment in extremely preterm infants. *Brain Behav Immun*. 2013;29:104-112. doi: 10.1016/j.bbi.2012.12.012 [doi].

40. Karve IP, Taylor JM, Crack PJ. The contribution of astrocytes and microglia to traumatic brain injury. *Br J Pharmacol*. 2015. doi: 10.1111/bph.13125 [doi].

41. Farraher SW, Jara H, Chang KJ, Hou A, Soto JA. Liver and spleen volumetry with quantitative MR imaging and dual-space clustering segmentation. *Radiology*. 2005;237(1):322-328. doi: 2371041416 [pii].

42. Watanabe M, Sakai O, Norbash AM, Jara H. Accurate brain volumetry with diffusion-weighted spin-echo single-shot echo-planar-imaging and dual-clustering segmentation: Comparison with volumetry-validated quantitative magnetic resonance imaging. *Med Phys*. 2010;37(3):1183-1190.

43. Bauer CM, Jara H, Killiany R, Alzheimer's Disease Neuroimaging Initiative. Whole brain quantitative T2 MRI across multiple scanners with dual echo FSE: Applications to AD, MCI, and normal aging. *Neuroimage*. 2010;52(2):508-514. doi: 10.1016/j.neuroimage.2010.04.255 [doi].

44. Saito N, Sakai O, Ozonoff A, Jara H. Relaxo-volumetric multispectral quantitative magnetic resonance imaging of the brain over the human lifespan: Global and regional aging patterns. *Magn Reson Imaging*. 2009;27(7):895-906. doi: 10.1016/j.mri.2009.05.006 [doi].

45. Suzuki S, Sakai O, Jara H. Combined volumetric T1, T2 and secular-T2 quantitative MRI of the brain: Age-related global changes (preliminary results). *Magn Reson Imaging*. 2006;24(7):877-887. doi: S0730-725X(06)00148-2 [pii].

46. Stewart AL, Rifkin L, Amess PN, et al. Brain structure and neurocognitive and behavioural function in adolescents who were born very preterm. *Lancet*. 1999;353(9165):1653-1657. doi: S014067369807130X [pii].

47. Olsen P, Vainionpaa L, Paakko E, Korkman M, Pyhtinen J, Jarvelin MR. Psychological findings in preterm children related to neurologic status and magnetic resonance imaging. *Pediatrics*. 1998;102(2 Pt 1):329-336.

48. de Vries LS, Eken P, Groenendaal F, van Haastert IC, Meiners LC. Correlation between the degree of periventricular leukomalacia diagnosed using cranial ultrasound and MRI later in infancy in children with cerebral palsy. *Neuropediatrics*. 1993;24(5):263-268. doi: 10.1055/s-2008-1071554 [doi].

49. Tolsa CB, Zimine S, Warfield SK, et al. Early alteration of structural and functional brain development in premature infants born with intrauterine growth restriction. *Pediatr Res*. 2004;56(1):132-138. doi: 10.1203/01.PDR.0000128983.54614.7E [doi].

50. Thompson DK, Warfield SK, Carlin JB, et al. Perinatal risk factors altering regional brain structure in the preterm infant. *Brain*. 2007;130(Pt 3):667-677. doi: awl277 [pii].

51. Inder T, Neil J, Yoder B, Rees S. Patterns of cerebral injury in a primate model of preterm birth and neonatal intensive care. *J Child Neurol*. 2005;20(12):965-967.

52. Cheong JL, Hunt RW, Anderson PJ, et al. Head growth in preterm infants: Correlation with magnetic resonance imaging and neurodevelopmental outcome. *Pediatrics*. 2008;121(6):e1534-40. doi: 10.1542/peds.2007-2671 [doi].

53. Kesler SR, Reiss AL, Vohr B, et al. Brain volume reductions within multiple cognitive systems in male preterm children at age twelve. *J Pediatr*. 2008;152(4):513-20, 520.e1. doi: 10.1016/j.jpeds.2007.08.009 [doi].

54. Giedd JN, Blumenthal J, Jeffries NO, et al. Brain development during childhood and adolescence: A longitudinal MRI study. *Nat Neurosci*. 1999;2(10):861-863. doi: 10.1038/13158 [doi].

55. Durston S, Hulshoff Pol HE, Casey BJ, Giedd JN, Buitelaar JK, van Engeland H. Anatomical MRI of the developing human brain: What have we learned? *J Am Acad Child Adolesc Psychiatry*. 2001;40(9):1012-1020. doi: S0890-8567(09)60442-1 [pii].

56. Reiss AL, Kesler SR, Vohr B, et al. Sex differences in cerebral volumes of 8-year-olds born preterm. *J Pediatr*. 2004;145(2):242-249. doi: 10.1016/j.jpeds.2004.04.031 [doi].

57. Volpe JJ. Brain injury in the premature infant--current concepts of pathogenesis and prevention. *Biol Neonate*. 1992;62(4):231-242.

58. Murphy DJ, Squier MV, Hope PL, Sellers S, Johnson A. Clinical associations and time of onset of cerebral white matter damage in very preterm babies. *Arch Dis Child Fetal Neonatal Ed*. 1996;75(1):F27-32.

59. Blakemore SJ, Choudhury S. Brain development during puberty: State of the science. *Dev Sci*. 2006;9(1):11-14. doi: DESC456 [pii].

60. Inder TE, Huppi PS, Warfield S, et al. Periventricular white matter injury in the premature infant is followed by reduced cerebral cortical gray matter volume at term. *Ann Neurol*. 1999;46(5):755-760.

61. Mashayekhi F, Draper CE, Bannister CM, Pourghasem M, Owen-Lynch PJ, Miyan JA. Deficient cortical development in the hydrocephalic texas (H-tx) rat: A role for CSF. *Brain*. 2002;125(Pt 8):1859-1874.

62. Miyan JA, Nabiyouni M, Zendah M. Development of the brain: A vital role for cerebrospinal fluid. *Can J Physiol Pharmacol*. 2003;81(4):317-328. doi: 10.1139/y03-027 [doi].

## CURRICULUM VITAE